



CrossMark
 click for updates

Cite this: *RSC Adv.*, 2015, 5, 65408

Suppression of coke formation and enhancement of aromatic hydrocarbon production in catalytic fast pyrolysis of cellulose over different zeolites: effects of pore structure and acidity

Pouya Sirous Rezaei, Hoda Shafaghat and Wan Mohd Ashri Wan Daud*

Rapid deactivation of zeolites caused by high formation and deposition of coke is a great challenge in catalytic conversion of biomass materials into value-added chemicals and fuels. The main purpose of this work was to reduce the formation of both types of thermal and catalytic coke over zeolites. It was revealed that there is a significant interaction between zeolite pore structure and the density of acid sites which could be optimized for reduced coke formation. In this study, catalytic pyrolysis of cellulose was conducted using HZSM-5 (Si/Al: 30), HY (Si/Al: 30) and physically mixed catalysts of HZSM-5 (Si/Al: 30) and dealuminated HY (Si/Al: 327). Coke formation over the physically mixed catalysts was remarkably lower than that over HZSM-5 and HY; the coke contents of HZSM-5, HY and physically mixed catalysts of HZSM-5 and dealuminated HY with a ratio of 70 : 30 wt% were 7.01, 11.47 and 4.82 wt%, respectively. The aromatic hydrocarbon yield was also considerably enhanced over the physically mixed catalysts compared to HZSM-5 and HY; the aromatic hydrocarbon yields achieved over HZSM-5, HY and the mixture of HZSM-5 and dealuminated HY (70 : 30 wt%) were 20.31, 8.91 and 27.01 wt%, respectively. This study shows that the interactive effects of zeolite characteristics such as pore structure and acidity could be taken into account for designing more efficient catalysts to achieve lower coke formation and higher production of desired products.

Received 14th June 2015
 Accepted 27th July 2015

DOI: 10.1039/c5ra11332f

www.rsc.org/advances

1. Introduction

The depletion of fossil fuels and the negative impacts of their utilization on the environment such as global warming and air pollution necessitate the discovery of renewable, sustainable and environmentally friendly alternative sources of energy.^{1–3} Lignocellulosic biomass is of great potential to be considered as such an alternative since it is abundantly available, and the fuel obtained from biomass is carbon dioxide neutral.⁴ Biomass pyrolysis which leads to a liquid product called bio-oil has gained extensive attention as an economically feasible technique for large-scale exploitation of biomass.⁵ However, bio-oil is highly oxygenated and has poor fuel properties such as high viscosity, poor heating value, corrosiveness, and chemical and thermal instability.^{6–9} It is also immiscible with conventional fossil fuels, and therefore needs to be upgraded. Catalytic pyrolysis is considered an efficient technology since it includes both steps of pyrolysis and catalytic upgrading in one unit. Zeolites have been the most common catalysts used for atmospheric pressure upgrading

of pyrolysis vapors in catalytic pyrolysis of biomass feedstocks. The major challenge in this process is high formation and deposition of coke on zeolite which causes high deactivation of catalyst.¹⁰ The reason for high yield of coke is low hydrogen to carbon effective ratio of biomass which leads to low hydrogen content in hydrocarbon pool inside catalyst. Coke deposited on catalyst is divided into two types of thermal and catalytic origin.¹¹ Thermal coke is produced by homogeneous thermal polymerization of compounds in gas phase, and is mainly deposited on outer surface of catalyst.¹² Catalytic coke is formed in the internal channels of catalyst as a result of heterogeneous transformation of oxygenate compounds over zeolite acid sites through reactions of oligomerization, cyclization, aromatization and condensation.^{13–15} Coke deposition results in catalyst deactivation through poisoning zeolite acid sites and pore blockage. In addition to catalyst deactivation, coke formation is a competing reaction with production of desired products. Therefore, it is essential to optimize catalyst properties in order to lower coke formation.

Zeolite pore structure and acidity are the two significant catalyst properties which greatly affect the amount of coke formation. In catalytic upgrading of pine wood pyrolysis vapors, it was revealed that among beta, Y and ferrierite zeolites,

Department of Chemical Engineering, Faculty of Engineering, University of Malaya, 50603 Kuala Lumpur, Malaysia. E-mail: pouya.sr@gmail.com; h.shafaghat@gmail.com; ashri@um.edu.my; Fax: +60 3 79675319; Tel: +60 3 79675297

ferrierite with too narrow pores led to less coke yield.¹⁶ Similarly, in catalytic pyrolysis of pine wood, it was reported that higher amount of coke was formed over the catalyst with higher pore size.¹⁷ Coke content of spent zeolites decreased in the order H-Y > H-beta > H-mordenite > HZSM-5. In another work for catalytic pyrolysis of wood biomass, catalysts with larger pore size resulted in higher coke yields; Y zeolite and activated alumina which contain larger pore size produced higher amount of coke compared to ZSM-5.¹⁸ It was declared that large coke precursors could diffuse into pore structure of catalysts with larger pore size and involve in coke formation. In catalytic pyrolysis of glucose using various zeolites with pores of different size and shape, the least amount of coke formation was observed over ZSM-5 and ZSM-11 with medium pore size, and the highest coke yield was obtained using beta zeolite, SSZ-55 and Y zeolite which had the largest pores.¹⁹ It was also shown that coke yield is a great function of the space inside zeolite channels; MCM-22, TNU-9 and IM-5 with medium pore size caused high amounts of coke due to their high internal pore space which provides enough space for coke formation. However, in contrast with what is mentioned above, Zhiqiang Ma *et al.*²⁰ concluded that lower yield of coke is formed over the catalyst with larger pore size, since larger pore size allows larger molecules to enter catalyst and react and not to be converted to thermal coke. In addition to pore size, other characteristics of pore structure of zeolites such as total porosity, pore shape, the amount of intercrystalline pores and connectivity of zeolite channels have also significant impact on the amount of coke formation. Pore shape could cause steric constraints for formation of the transition states which are involved in production of coke precursors.²¹ Meso- and macropores between zeolite crystals allow high degree of polymerization resulting in the growth of coke.^{22,23} Three-dimensional porous structure could reduce coke formation due to high connectivity of channels which results in enhanced movement of coke precursor intermediates to the outside of zeolite crystals.²⁴ Apart from pore structure, zeolite acidity is also influential on the amount of coke formation. Since catalytic coke is formed over zeolite acid sites, its yield is dependent on strength distribution and density of acid sites. Catalytic coke content of zeolite is expected to be increased by increase in strength and number of acid sites.

In this work, the interactive effects of zeolite pore structure and density of acid sites on coke formation was investigated. Cellulose which is the most abundant organic polymer in nature was used as feedstock. The main purpose of this study was to enhance the yield of aromatic hydrocarbons and to suppress coke formation in catalytic pyrolysis of cellulose using a physically mixed catalyst system. Since aromatic hydrocarbons have wide range of applications and are the building blocks for petrochemical industry, these highly desirable compounds are usually considered as target products in catalytic conversion of biomass derived feedstocks.^{10,25,26} HZSM-5, HY and mixtures of HZSM-5 and dealuminated HY were used as catalyst.

2. Experimental

2.1. Catalyst preparation

HZSM-5, HY (Zeolyst, CBV 720, SiO₂/Al₂O₃ molar ratio: 30) and mixtures of HZSM-5 and dealuminated HY were used for catalytic pyrolysis of cellulose (Acros Organics) in this work. HZSM-5 was obtained by calcination of the ammonium form of ZSM-5 (Zeolyst, CBV 3024E, SiO₂/Al₂O₃ molar ratio: 30) at 550 °C (with heating rate of 3 °C min⁻¹) for 12 h. The dealuminated HY was obtained by treatment of HY in 2 M aqueous HCl solution at 80 °C for 12 h using 15 ml acid solution/g_{zeolite}. Then, the sample was filtered, washed with distilled water, and dried at 100 °C for 12 h. Afterward, the dealuminated sample was converted to the protonic form by ion exchange in 0.1 M aqueous NH₄Cl solution at 60 °C for 12 h using 50 ml NH₄Cl solution/g_{zeolite}, followed by calcination at 550 °C for 12 h.

2.2. Catalyst characterization

The crystallinity of zeolites was determined by X-ray diffraction (XRD) on a Rigaku Miniflex diffractometer using Cu K α radiation ($\lambda = 1.54443 \text{ \AA}$) at 45 kV and 40 mA. Data were recorded in the 2θ range of 5–80° with a step size of 0.026° and scan rate of 0.05° s⁻¹. X-ray fluorescence (XRF) instrument (PANalytical AxiosmAX) was used for chemical analysis of catalysts. The surface area and pore size distribution of catalysts were determined by N₂ isothermal (–196 °C) adsorption–desorption using Micromeritics ASAP 2020 surface area and porosity analyzer. Prior to the analysis, the samples were degassed in vacuum at 180 °C for 4 h. Characterization of acid site distribution of the catalysts was conducted by temperature programmed desorption of ammonia (NH₃-TPD) using Micromeritics ChemiSorb 2720 instrument. Using He as carrier gas (20 ml min⁻¹), 200 mg of each sample set in TPD cell was heated from ambient temperature to 600 °C at a heating rate of 20 °C min⁻¹ and maintained at 600 °C for 1 h. Afterward, the sample was cooled to 210 °C and purged with 10% NH₃/90% He mixture (20 ml min⁻¹) for 30 min. Then, the sample was flushed with He gas for 30 min for removal of physisorbed ammonia. After cooling down to 70 °C and when the thermal conductivity detector (TCD) signal was stable, ammonia desorption measurement was performed by heating the sample to 600 °C at a rate of 10 °C min⁻¹ under He flow (20 ml min⁻¹). The coke content of spent catalysts was measured by thermogravimetric analysis using a PerkinElmer STA 6000 Simultaneous Thermal Analyzer. Under synthetic air flow (100 ml min⁻¹), samples were heated from 30 to 750 °C at the rate of 5 °C min⁻¹ and kept at final temperature for 30 min.

2.3. Catalytic activity measurement

Catalytic pyrolysis was carried out in a continuous, down-flow, fixed-bed tubular reactor (ID: 7.5 cm; height: 60 cm) made of stainless steel 316L which was placed coaxially in a two-zone furnace. A stainless steel cylindrical cup with screen of 400 mesh at the bottom side was set in each zone of the reactor. In each run, 5 g calcined catalyst was loaded in the second cup (ID: 2.5 cm; height: 5 cm), and cellulose was fed into the first cup

through a feed hopper on the top of the reactor. The first zone was used for pyrolysis, and the pyrolysis vapors were passed through catalyst bed in the second cup for catalytic upgrading. All runs were conducted at atmospheric pressure. Temperature of each zone was measured by a K-type thermocouple. Both zones were heated to 500 °C and nitrogen (Linde Malaysia Sdn. Bhd.) was purged to the reactor at flow rate of 2 L min⁻¹ for 30 min. Afterward, 30 g cellulose was introduced to the reactor with weight hourly space velocity (WHSV) of 6 h⁻¹ and N₂ flow rate was kept at 2 L min⁻¹. The liquid products were collected by two condensers maintained at -10 °C. All lines were heated to avoid any condensation. After each run, the catalyst bed was purged by N₂ flow (2 L min⁻¹) at the reaction temperature for 30 min in order to eliminate the components which might remain on the catalyst. The organic phase of liquid product was separated from the aqueous phase with ethyl acetate (R&M chemicals) before injection to GC/MS. Qualitative and quantitative analysis of liquid products was carried out by GC/MS (Shimadzu QP 2010, DB-5 30 m × 0.25 mm × 0.25 μm), equipped with flame ionization and mass spectrometry detection. The GC oven temperature program was as follows: temperature was held at 50 °C for 5 min, ramped to 300 °C at 10 °C min⁻¹, and kept at 300 °C for 10 min. The injector temperature was 290 °C and a split ratio of 50 : 1 was employed. Helium (Linde Malaysia Sdn. Bhd) was used as carrier gas with flow rate of 1.26 ml min⁻¹. NIST (National Institute of Standards and Technology) mass spectrum library was used for peak identification. 2-Isopropylphenol (Sigma-Aldrich) was used as internal standard for quantitative analysis of products. Yield and selectivity of products were calculated as follows: yield = (weight of a certain product/total weight of feed) × 100; selectivity = (weight of a certain product/total weight of organic phase in liquid product) × 100.

3. Results and discussion

3.1. Physicochemical characteristics of catalysts

The acidity of catalysts determined by NH₃-TPD analysis is shown in Fig. 1. The lower peak area of acid-treated HY compared to that of parent HY demonstrates the reduction in the number of acid sites caused by leaching of Al from zeolite structure. SiO₂/Al₂O₃ molar ratio of the parent and dealuminated forms of HY were 31.3 and 326.7, respectively. As depicted in Fig. 2, both parent and dealuminated forms of HY displayed the typical diffraction lines of Y zeolite. It can be seen from XRD patterns that crystallinity of acid-treated HY had a slight reduction, and crystalline structure of HY was not significantly affected by dealumination. Table 1 presents the textural properties of catalysts evaluated from nitrogen isothermal adsorption-desorption. BET surface area of dealuminated HY was 13% lower than that of parent HY. Microporous surface area and volume of HY were reduced, while surface area and volume of mesopores were increased. This indicates that a portion of micropores was changed to mesopores due to extraction of aluminium from zeolite microporous channels and creation of mesoporous space. As shown in Fig. 3, all zeolites displayed type IV isotherm. HZSM-5 and parent HY

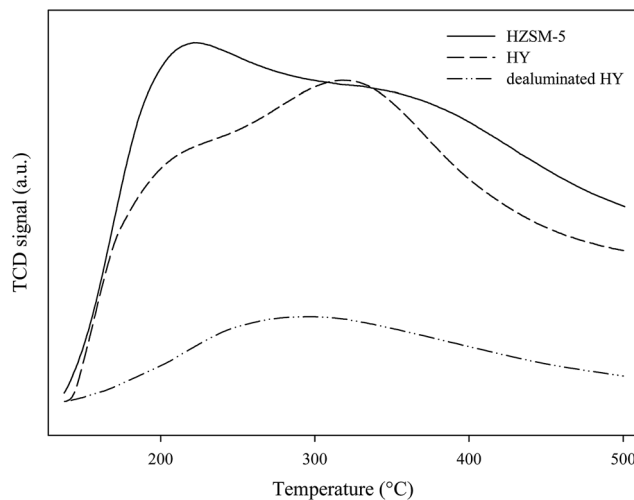


Fig. 1 NH₃-TPD profiles of HZSM-5 and the parent and dealuminated forms of HY.

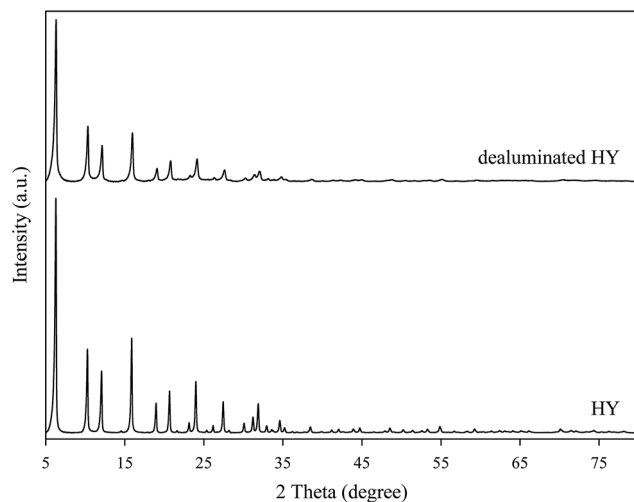


Fig. 2 X-ray diffraction patterns of the parent and dealuminated forms of HY.

displayed H4-type hysteresis loop associated with narrow slit-shaped pores, and dealuminated HY exhibited H3-type hysteresis loop associated with slit-shaped pores.²⁷

3.2. Catalytic pyrolysis of cellulose over HZSM-5 and HY

Table 2 presents the yields of gas, liquid and solid products obtained from catalytic pyrolysis of cellulose using different zeolites. HZSM-5 resulted in lower yield of oil as well as higher yields of gas and water compared to HY due to higher amount of deoxygenation taken place over HZSM-5. As shown in Table 2, the aromatic hydrocarbons yield achieved from catalytic pyrolysis of cellulose over HZSM-5 and HY were 20.31 and 8.91 wt%, respectively. The higher aromatic hydrocarbons yield of HZSM-5 compared to HY is due to the different pore structures of these catalysts. ZSM-5 is a zeolite with three-dimensional framework formed of 10-membered ring pores with dimensions of 0.51 ×

Table 1 Chemical and textural properties of catalysts

Sample	SiO ₂ /Al ₂ O ₃ ^a	S _{BET} ^b (m ² g ⁻¹)	S _{meso} ^c (m ² g ⁻¹)	S _{BET} /S _{meso}	V _{total} ^d (cm ³ g ⁻¹)	V _{micro} ^e (cm ³ g ⁻¹)	V _{meso} ^f (cm ³ g ⁻¹)
HZSM-5	32.3	291	99	2.94	0.191	0.094	0.097
Parent HY	31.3	645	158	4.08	0.429	0.238	0.191
Dealuminated HY	326.7	563	256	2.19	0.431	0.149	0.282

^a Determined by XRF analysis. ^b Calculated in the range of relative pressure (P/P_0) = 0.05 – 0.25. ^c Evaluated by *t*-plot method. ^d Total pore volume evaluated at $P/P_0 = 0.99$. ^e Evaluated by *t*-plot method. ^f $V_{meso} = V_{total} - V_{micro}$.

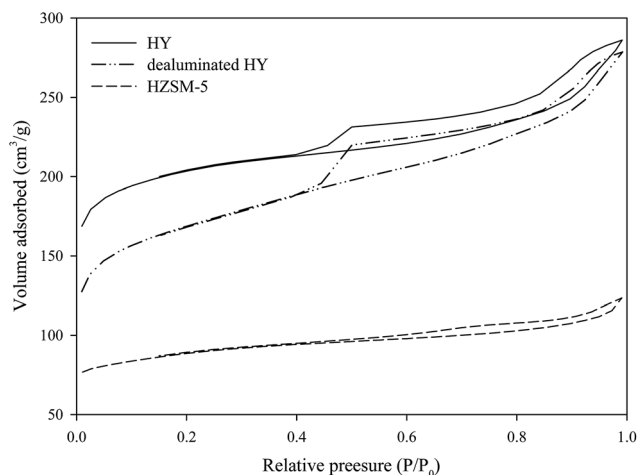


Fig. 3 Nitrogen adsorption–desorption isotherms of HZSM-5 and the parent and dealuminated forms of HY.

0.55 and 0.53×0.56 nm, while Y zeolite contains 12-membered ring channels of 0.74×0.74 nm.¹⁹ The smaller pore size of HZSM-5 prevents from formation of polyaromatic compounds

which act as coke precursors, resulting in lower deposition of catalytic coke on HZSM-5 acid sites, and in turn, less deactivation of catalyst and higher yield of aromatic hydrocarbons.²⁸ The main aromatic hydrocarbons produced from cellulose pyrolysis over HZSM-5 were toluene, xylene, trimethylbenzene and ethyl-methylbenzene. The dominant oxygenated compounds detected in the organic phase of liquid product obtained using HZSM-5 and HY were furfural, benzofuran, 5-hydroxymethyl furfural, phenol, cresol and benzenediol. The reaction pathway for conversion of cellulose into aromatic hydrocarbons is as follows: pyrolysis of cellulose to volatile organics which are dehydrated to furans, followed by decarbonylation of furans to allene, and subsequent oligomerization of the allene to olefins which react with furans to form aromatics.^{29,30} In addition to lower yield of aromatic hydrocarbons, HY resulted in higher coke formation compared to HZSM-5; the content of coke deposited on HZSM-5 and HY were 7.01 and 11.47 wt%, respectively. Besides, the main cause of coke formation over these two zeolites was different. The results obtained by thermogravimetric analysis of spent catalysts shown in Fig. 4a and Table 3 depict that the coke deposited on HZSM-5 is mostly of thermal origin and the coke formed over

Table 2 Product yields and selectivities (wt%) obtained from catalytic pyrolysis of cellulose over different zeolites. Reaction conditions: WHSV, 6 h⁻¹; reaction temperature, 500 °C; pressure, 1 atm

Catalyst	HZSM-5	HY	Dealuminated HY	HZSM-5/dealuminated HY		
				70 : 30 wt%	50 : 50 wt%	30 : 70 wt%
% Yield						
Oil	27.96	31.85	37.59	28.98	30.28	31.22
Gas	33.74	29.73	27.17	33.46	32.86	32.26
Aqueous fraction	17.46	15.95	14.65	17.30	16.71	16.49
Char/coke	19.57/1.27	20.30/2.17	19.86/0.73	19.43/0.83	19.38/0.77	19.30/0.73
% Yield of aromatic hydrocarbons						
	20.31	8.91	0.48	27.01	22.18	15.71
% Selectivity in organic phase of liquid product						
Benzene	1.36	0.30	0.09	2.01	1.17	0.71
Toluene	19.47	5.72	0.23	26.28	18.45	11.49
Xylene	17.08	6.82	0.27	24.8	16.85	10.65
Ethyl-methylbenzene	7.53	3.07	0.13	11.64	8.85	6.65
Trimethylbenzene	9.91	4.22	0.16	13.75	11.24	8.06
Tetramethylbenzene	2.86	1.46	0.11	1.97	2.18	1.21
Naphthalenes	9.24	4.84	0.19	8.40	9.68	6.5
Other hydrocarbons	5.19	1.54	0.10	4.35	4.83	5.05
Oxygenated compounds	27.36	72.03	98.72	6.80	26.75	49.68

HY is mostly of catalytic origin; HZSM-5 and HY resulted in catalytic coke content of 2.28 and 10.21 wt%, and thermal coke content of 4.73 and 1.26 wt%, respectively. The two weight loss regions in temperature range of 300–500 and 500–750 °C were considered as the amounts of thermal and catalytic coke deposited on catalyst, respectively. The weight loss below 300 °C was assigned to desorption of water and volatile components.²⁰ Differential thermogravimetry (DTG) shown in Fig. 4b indicates that maximum combustion of thermal and catalytic coke was occurred at 440 and 580 °C for HZSM-5, and 410 and 650 °C for HY, respectively. The difference in catalytic and thermal coke contents of HZSM-5 and HY is caused by the different pore structures of these two zeolites. In fact, coke formation is a shape selective reaction. Large molecules formed by thermal cracking in homogeneous gas phase outside catalyst could not enter the narrow channels of HZSM-5 and undergo repolymerization and condensation outside catalyst, and are deposited

on catalyst surface as thermal coke. However, HY which contains larger channels allows larger molecules enter the catalyst and react over zeolite acid sites inside catalyst channels. On the other hand, HY leads to higher yield of catalytic coke since this zeolite with larger pore diameter provides larger space for polymerization of coke precursors and formation of the intermediates and transition states which are involved in coke production resulting in higher amount of carbonaceous residues deposited on zeolite acid sites. In contrast to HY, smaller channels of HZSM-5 limit the degree of polymerization inside catalyst and cause lower yield of catalytic coke.

3.3. Catalytic pyrolysis of cellulose over physically mixed catalysts of HZSM-5 and dealuminated HY

The amount of catalytic coke formed over HY was remarkably reduced by dealumination. The catalytic coke contents of HY and dealuminated HY were 10.21 and 3.08 wt%, respectively. Huifu Xue *et al.*²⁷ also reported that dealumination resulted in less deposition of catalytic coke on mordenite zeolite. Dealuminated HY contains lower density of acid sites which leads to lower yield of catalytic coke. High molecular coke is formed through several reaction steps, and since lower density of acid sites leads to reduction in the number of acid sites which a reactant encounters, the possibility for converting into coke over dealuminated HY is attenuated. However, the aromatics yield achieved over dealuminated HY was very low (below 0.5 wt%). Use of mixtures of HZSM-5 and dealuminated HY showed to be efficient to achieve high yield of aromatic hydrocarbons with low content of coke deposited on catalyst. The coke contents of HZSM-5 and HY were 7.01 and 11.47 wt%, while the coke contents of mixtures of HZSM-5 and dealuminated HY with ratios of 70 : 30, 50 : 50 and 30 : 70 wt% were 4.82, 4.38 and 4.17 wt%, respectively. In the case of using HZSM-5 as catalyst, the compounds with molecular size larger than pore diameter of HZSM-5 could not enter catalyst and are converted to thermal coke and deposited on HZSM-5 outer surface. However, presence of HY with larger channels in catalyst mixture allows the compounds in wider range of molecular size to diffuse into catalyst and react over HY acid sites. In fact, the dealuminated HY showed to be a suitable catalyst for initial cracking of the compounds derived from pyrolysis of cellulose. Therefore, some compounds which could not enter HZSM-5 are firstly cracked over HY acid sites and converted to smaller compounds which could diffuse inside HZSM-5 channels and

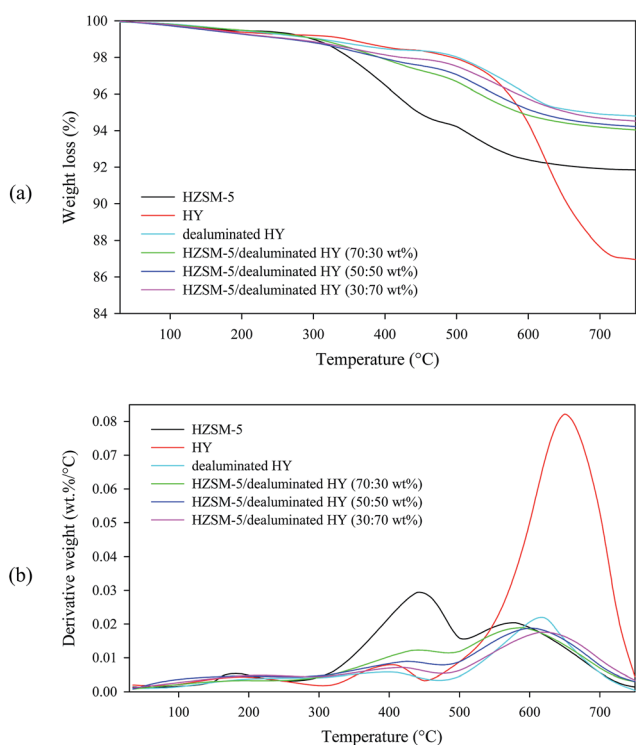


Fig. 4 TGA (a) and DTG (b) of the spent catalysts used for cellulose pyrolysis (WHSV, 6 h⁻¹; time on stream, 60 min; reaction temperature, 500 °C).

Table 3 Content of total coke, thermal coke and catalytic coke deposited on the catalysts used for cellulose pyrolysis. Reaction conditions: WHSV, 6 h⁻¹; reaction temperature, 500 °C; pressure, 1 atm; time on stream, 60 min

Catalyst	HZSM-5	HY	Dealuminated HY	HZSM-5/dealuminated HY		
				70 : 30 wt%	50 : 50 wt%	30 : 70 wt%
% g _{coke} /g _{catalyst}						
Thermal coke	4.73	1.26	1.07	2.36	1.73	1.38
Catalytic coke	2.28	10.21	3.08	2.46	2.65	2.79
Total coke	7.01	11.47	4.15	4.82	4.38	4.17

be transformed to aromatic hydrocarbons over HZSM-5 acid sites. Considering the thermal coke contents of the mixtures of HZSM-5 and dealuminated HY shown in Table 3 as well as the thermal coke content of dealuminated HY which is 1.07 wt% (thermal coke content of dealuminated HY is supposed to be unchanged in presence of HZSM-5), the thermal coke content of HZSM-5 in mixtures of HZSM-5 and dealuminated HY with ratios of 70 : 30, 50 : 50 and 30 : 70 wt% are estimated to be 2.91, 2.39 and 2.10 wt%, respectively. This clearly shows that thermal coke content of HZSM-5 is reduced by increase in the amount of dealuminated HY in catalyst mixture. Meanwhile, dealuminated HY does not contain enough number of acid sites for high conversion of reactants to coke. Therefore, mixture of HZSM-5 and dealuminated HY results in less coke formation compared to HZSM-5 and HY due to the reduction in thermal coke deposited on HZSM-5 and the decrease in catalytic coke formed inside the channels of dealuminated HY. It could be inferred from the results obtained in this study that there is a significant interaction between pore space and density of zeolite acid sites which should be taken into account in designing an efficient catalyst. The steric constraints caused by limited space in the vicinity of acid sites could prevent from coke formation. Therefore, high density of acid sites located in small spaces could not lead to high formation of coke. However in larger channels, coke formation could be effectively suppressed by decrease in the density of acid sites which leads to reduction in the degree of polymerization and condensation. The aromatic hydrocarbons production is also improved over the physically mixed catalyst system. The aromatics yield achieved over HZSM-5 was 20.31 wt% which was enhanced to 22.18 and 27.01 wt% over mixtures of HZSM-5 and dealuminated HY with ratios of 50 : 50 and 70 : 30 wt%, respectively. This increase in aromatics yield is due to the possibility for a higher fraction of compounds to react over HZSM-5 since the compounds with molecular size larger than pore diameter of HZSM-5 could undergo cracking in larger channels of HY and diffuse inside HZSM-5 channels. However, the mixture of HZSM-5 and dealuminated HY with ratio of 30 : 70 wt% resulted in less aromatics yield compared to HZSM-5 illustrating that the amount of HZSM-5 in the catalyst mixture should be adequate in order to proceed the reactions required for aromatics production; as mentioned in the previous section, formation of polyaromatic compounds as coke precursors is restricted by the steric constraints caused by smaller pore size of HZSM-5 resulting in higher catalytic activity of HZSM-5 and higher yield of aromatic hydrocarbons produced over this catalyst compared to HY. Therefore in the mixture of HZSM-5 and dealuminated HY, the amount of dealuminated HY should be sufficient for initial cracking of pyrolysis-derived compounds and effective reduction of thermal coke deposited on HZSM-5. Besides, the amount of HZSM-5 in the mixture should be high enough for efficient conversion of reactants. In the physically mixed catalyst system studied in this work, the lowest coke formation and the highest yield of aromatic hydrocarbons were observed at HZSM-5 to dealuminated HY ratios of 30 : 70 and 70 : 30 wt%, respectively.

It could be concluded from this study that formation of coke as an undesired product is a competing reaction with

production of aromatic hydrocarbons in catalytic pyrolysis of biomass feedstocks. Therefore, catalyst properties should be optimized in order to have minimum selectivity towards coke and maximum selectivity towards desired products. Deposition of both types of coke is needed to be suppressed in an efficient catalyst system. Pore structure and location of acid sites in catalyst structure are the two significant properties which should be taken into account for reducing coke formation. Presence of channels with larger dimensions facilitates the diffusion of larger molecules inside catalyst leading to reduction in the yield of thermal coke. Meanwhile, acid sites with high density should be located in small spaces which restrict the degree of polymerization and catalytic coke deposition. However, there should be enough space in the vicinity of acid sites in order to allow formation of transition states for desired products.

4. Conclusions

The results obtained in this study revealed that there is a significant interaction between zeolite pore structure (pore size and shape) and density of acid sites which greatly affects the amount of coke formation and deposition on zeolite in conversion of biomass feedstocks. It was also shown that these zeolite properties could be optimized in order to suppress coke formation and to enhance the yield of desired products. In catalytic pyrolysis of cellulose, lower formation of coke as well as higher yield of aromatic hydrocarbons were achieved over physically mixed catalysts of HZSM-5 and dealuminated HY compared to HZSM-5 and HY. Addition of HY to HZSM-5 results in lower deposition of thermal coke over HZSM-5 due to larger pores of HY which allow larger molecules diffuse into zeolite and react. Besides, formation of catalytic coke over the physically mixed catalysts was suppressed by small space inside HZSM-5 pores and low density of acid sites inside dealuminated HY pores which both restrict the degree of polymerization of coke precursors. The coke contents of HZSM-5 and HY were 7.01 and 11.47 wt%, respectively, while the coke content of physically mixed catalysts of HZSM-5 and dealuminated HY with ratio of 70 : 30 wt% was 4.82 wt%. Meanwhile, The aromatic hydrocarbons yield achieved over HZSM-5 and HY was 20.31 and 8.91 wt%, respectively, which was enhanced to 27.01 wt% over mixture of HZSM-5 and dealuminated HY (70 : 30 wt%).

Acknowledgements

This work was conducted with the financial support of the Faculty of Engineering at University of Malaya through the HIR Grant (D000011-16001).

References

- 1 C. Perego and A. Bosetti, *Microporous Mesoporous Mater.*, 2011, **144**, 28–39.
- 2 K. C. Kwon, H. Mayfield, T. Marolla, B. Nichols and M. Mashburn, *Renewable Energy*, 2011, **36**, 907–915.

- 3 J. C. Serrano-Ruiz and J. A. Dumesic, *Energy Environ. Sci.*, 2011, **4**, 83–99.
- 4 Q. Zhang, J. Chang, T. Wang and Y. Xu, *Energy Fuels*, 2006, **20**, 2717–2720.
- 5 Y. Zhang, T. R. Brown, G. Hu and R. C. Brown, *Chem. Eng. J.*, 2013, **225**, 895–904.
- 6 W. Yu, Y. Tang, L. Mo, P. Chen, H. Lou and X. Zheng, *Bioresour. Technol.*, 2011, **102**, 8241–8246.
- 7 M. A. Peralta, T. Sooknoi, T. Danuthai and D. E. Resasco, *J. Mol. Catal. A: Chem.*, 2009, **312**, 78–86.
- 8 M. Song, Z. Zhong and J. Dai, *J. Anal. Appl. Pyrolysis*, 2010, **89**, 166–170.
- 9 H. Zhang, R. Xiao, H. Huang and G. Xiao, *Bioresour. Technol.*, 2009, **100**, 1428–1434.
- 10 P. S. Rezaei, H. Shafaghat and W. M. A. W. Daud, *Appl. Catal., A*, 2014, **469**, 490–511.
- 11 A. G. Gayubo, B. Valle, A. T. Aguayo, M. Olazar and J. Bilbao, *J. Chem. Technol. Biotechnol.*, 2010, **85**, 132–144.
- 12 T. R. Carlson, T. P. Vispute and G. W. Huber, *ChemSusChem*, 2008, **1**, 397–400.
- 13 A. G. Gayubo, B. Valle, A. T. Aguayo, M. Olazar and J. Bilbao, *Ind. Eng. Chem. Res.*, 2010, **49**, 123–131.
- 14 A. G. Gayubo, B. Valle, A. T. Aguayo, M. Olazar and J. Bilbao, *Energy Fuels*, 2009, **23**, 4129–4136.
- 15 A. G. Gayubo, A. T. Aguayo, A. Atutxa, R. Prieto and J. Bilbao, *Energy Fuels*, 2004, **18**, 1640–1647.
- 16 A. Aho, N. Kumar, A. V. Lashkul, K. Eränen, M. Ziolek, P. Decyk, T. Salmi, B. Holmbom, M. Hupa and D. Y. Murzin, *Fuel*, 2010, **89**, 1992–2000.
- 17 A. Aho, N. Kumar, K. Eränen, T. Salmi, M. Hupa and D. Y. Murzin, *Fuel*, 2008, **87**, 2493–2501.
- 18 P. T. Williams and P. A. Horne, *J. Anal. Appl. Pyrolysis*, 1995, **31**, 39–61.
- 19 J. Jae, G. A. Tompsett, A. J. Foster, K. D. Hammond, S. M. Auerbach, R. F. Lobo and G. W. Huber, *J. Catal.*, 2011, **279**, 257–268.
- 20 Z. Ma, E. Troussard and J. A. van Bokhoven, *Appl. Catal., A*, 2012, **423–424**, 130–136.
- 21 H. Zhang, Y.-T. Cheng, T. P. Vispute, R. Xiao and G. W. Huber, *Energy Environ. Sci.*, 2011, **4**, 2297–2307.
- 22 B. Valle, P. Castaño, M. Olazar, J. Bilbao and A. G. Gayubo, *J. Catal.*, 2012, **285**, 304–314.
- 23 P. M. Mortensen, J. D. Grunwaldt, P. A. Jensen, K. G. Knudsen and A. D. Jensen, *Appl. Catal., A*, 2011, **407**, 1–19.
- 24 M. Ibáñez, B. Valle, J. Bilbao, A. G. Gayubo and P. Castaño, *Catal. Today*, 2012, **195**, 106–113.
- 25 Z. Du, X. Ma, Y. Li, P. Chen, Y. Liu, X. Lin, H. Lei and R. Ruan, *Bioresour. Technol.*, 2013, **139**, 397–401.
- 26 B. Zhang, Z. Zhong, M. Min, K. Ding, Q. Xie and R. Ruan, *Bioresour. Technol.*, 2015, **189**, 30–35.
- 27 H. Xue, X. Huang, E. Zhan, M. Ma and W. Shen, *Catal. Commun.*, 2013, **37**, 75–79.
- 28 A. Corma, G. Huber, L. Sauvanaud and P. Oconnor, *J. Catal.*, 2007, **247**, 307–327.
- 29 T. R. Carlson, G. A. Tompsett, W. C. Conner and G. W. Huber, *Top. Catal.*, 2009, **52**, 241–252.
- 30 Y. T. Cheng, J. Jae, J. Shi, W. Fan and G. W. Huber, *Angew. Chem., Int. Ed.*, 2012, **51**, 1387–1390.